

Pieter Blom M JSCE Hokkaido River Disaster Prevention Research Center

Introduction.

Hydraulic engineering structures have to be protected against local-scour, because local-scour can lead to undermining and the collapse of the structures. Local-scour holes are caused by non-equilibrium sediment transport. Downstream from structures the sediment particles are eroded, yielding local-scour holes, upstream from structures sediment particles are deposited, yielding a bottom level rise.

The prediction of local-scour holes is important in the design of hydraulic structures, because complete protection against scour is generally too expensive. In this study a model is presented to predict local-scour holes. It deals with clear-water scour downstream from structures. This means that the sediment transport in the flow is zero at the downstream-side of the structure, which is the upstream-side of the scour area.

The research concerning scour-holes started in the early sixties by deriving empirical relations from experiments in flumes. In later years, these coefficients were readjusted taking two- and three-dimensional (2DV and 3D) scour experiments into account (De Graauw & Pilarczyk, 1981). In the late seventies the first mathematical models were developed. Kerssens et al. (1979) presented a model to calculate morphological processes in gradually varying flows. Van Rijn (1986) extended this model by improving the computations of the velocities and the eddy-viscosity. Hoffmans (1992) developed a morphological model based on the 2DV Navier-Stokes and convection-diffusion equations. In this model the sediment transport was described using a stochastic approach for the bed-shear stress. Unfortunately, this model uses a prescribed eddy-viscosity. The present study is an extension of this model, using a $k\epsilon$ turbulence-model instead of a prescribed eddy-viscosity.

Numerical model.

The adaption of the velocity field is fast compared to the morphological process. Therefore, the velocity field in the morphological calculations can be considered as quasi-steady. This means that a numerical model can be split into a flow model to calculate the velocities and a morphological model to calculate the sediment transport. In this study the flow model used was PHOENICS of CHAM Ltd, the morphological model used was SUSTRA of Delft Hydraulics (Van Rijn & Meyer, 1986).

The flow model PHOENICS.

The 2DV steady calculations to obtain the velocities, eddy-viscosities, turbulence energy and bed shear stresses are made with the PHOENICS flow-simulation system. The equations solved in PHOENICS have the form:

$$\frac{\partial}{\partial t}(\rho \phi) + \nabla \cdot (\rho \vec{v} \phi - \Gamma_\phi \nabla \phi) = S_\phi \quad (1)$$

in which t is the time, ρ is the density, ϕ is any conserved property (for this model: mass fraction, the momentum per unit mass, turbulence energy (k) and dissipation of turbulence energy (ϵ)), \vec{v} is the velocity vector, Γ_ϕ is the diffusivity and S_ϕ is a source rate of ϕ . The boundary conditions used are the ordinary ones for $k\epsilon$ turbulence-models, which means: prescribed values for the bottom friction, k and ϵ at the bottom; a symmetry condition for k and a prescribed value for ϵ at the water surface. The vertical velocity could be taken zero at the water surface due to the rigid-lid assumption.

The morphological model SUSTRA.

The 2DV calculations to obtain the sediment transport are made with the SUSTRA-model. This model solves the convection-diffusion equation, having the form:

$$\frac{\partial \bar{u} \bar{c}}{\partial x} + \frac{\partial (\bar{w} - w_s) \bar{c}}{\partial z} = \frac{\partial}{\partial x} \left(\Gamma_x \frac{\partial \bar{c}}{\partial x} \right) + \frac{\partial}{\partial z} \left(\Gamma_z \frac{\partial \bar{c}}{\partial z} \right) \quad (2)$$

in which \bar{u} , \bar{c} and \bar{w} are the time-averaged horizontal velocity, concentration and vertical velocity, respectively, w_s is the particle fall velocity and Γ_x and Γ_z are the horizontal and vertical diffusivities. The horizontal diffusivity is assumed to be zero, while the vertical diffusivity is related to eddy-viscosity (ν) as (Van Rijn, 1984):

$$\nu = \beta \Gamma_z, \quad \beta = 1 + 2(w_s/u_*)^2 \quad (3)$$

in which u_* is the friction velocity. The boundary conditions used are: a zero concentration at the water surface, and a prescribed value for the concentration at a reference level close to the bed (\bar{c}_a). The concentration \bar{c}_a is determined using a stochastic approach, assuming Gaussian distributions of the probability distributions for as well the critical bed shear stress (related to the grains) and $\bar{\tau}_0$ the mean bed shear stress (related to the flow). According to Hoffmans (1992) $\hat{\tau}_{Gc}$ is about 1.5 times larger than the mean critical Shields value:

$$\hat{\tau}_{Gc} = \bar{\tau}_G - \delta_1 \sigma_c \leq \bar{\tau}_0 + \delta_1 \sigma_o = \hat{\tau}_{0c} \quad (4)$$

in which δ_1 is a constant and σ_c and σ_o are the standard deviations of $\hat{\tau}_{Gc}$ and $\hat{\tau}_{0c}$, respectively, $\bar{\tau}_G$ is the mean critical bed shear stress (related to the grains) and $\bar{\tau}_0$ the mean bed shear stress (related to the flow). According to Hoffmans (1992) $\hat{\tau}_{Gc}$ is about 1.5 times larger than the mean critical Shields value.

Turbulence parameters.

In this study the influence of the turbulence generated in the flow on the near bed concentration is expressed by the standard deviation (σ_i) of the mean bed shear-stress and calculated from PHOENICS results. In the recirculation zone the turbulence energy near the bed (k_b) appears to be much larger than the bed generated turbulence ($k_0 = u_*^2 / \sqrt{c_\mu}$), because the turbulence generated in the mixing layer (k_m) is convected along the bed. It is assumed that k_b is the average of the turbulence energy generated directly at the bed and the turbulence energy generated

by the mixing layer.

$$k_p(x) = \delta'_2 k_m(x) + \delta_2 k_0 \quad (5)$$

in which δ'_2 and δ_2 are coefficients. On the analogy of the standard deviation for uniform-flow conditions the standard deviation σ_i can be expressed in terms of turbulence energy (Hoffmans 1992):

$$\sigma_i(x) = \delta'_3 k_m(x) + \delta_3 k_0(x) \quad (6)$$

in which δ'_3 and δ_3 are coefficients and k_m is the depth-averaged turbulence energy.

Stochastic entrainment-parameter.

This parameter (E_m) was introduced by Van Rijn (1986). It is a measure for the total movement of the sediment particles: the bed load and the depth-averaged suspended load. The bed load is dependent on the direction of the instantaneous bed shear stresses and the transport-stage parameter (T_m). Therefore, the stochastic entrainment-parameter is split up in two parts, a contribution due to positive velocities (E_{m1}) and a contribution due to velocities against the main flow direction (E_{m2}):

$$E_{m1}(\gamma) = \int_0^{\infty} (T_m(\tau'_0))^{\gamma} P(\tau'_0) d\tau'_0, \quad E_{m2}(\gamma) = \int_{-\infty}^0 (T_m(\tau'_0))^{\gamma} P(\tau'_0) d\tau'_0 \quad (7)$$

where P is the probability distribution of the effective instantaneous bed shear stresses (τ'_0), which is assumed to be normally distributed:

$$P(\tau'_0) = \frac{1}{\sqrt{2\pi}\sigma_i} \exp\left(-\frac{(\tau'_0 - \bar{\tau}'_0)^2}{2\sigma_i^2}\right) \quad (8)$$

in which $\bar{\tau}'_0 = \mu \rho u_*^2$ is the mean effective bed shears-stress, $\tau'_0 = \mu \tau_0$ is the effective instantaneous bed shears-stress, $\mu = (C/C')^2$ is an efficiency factor, C is the overall Chézy-coefficient, C' is the grains related Chézy-coefficient and the parameter γ is between 1.5 to 2.1.

Bed concentration and bed load.

Using the stochastic entrainment-parameter, the time-averaged concentration at the reference level and the movement of sediment particles below the reference level (bed load) for uniform flow-conditions can be calculated. According to Hoffmans (1992) the equations for the bed load (S_b) and the reference concentration (\bar{c}_a) are:

$$S_b = 0.1 d_{50} \sqrt{\Delta g d_{50}} \frac{E_{m1}(2.1) - E_{m2}(2.1)}{D_*^{0.3}}, \quad \bar{c}_a = 0.03 \frac{d_{50}}{a} \frac{E_{m1}(1.5) + E_{m2}(1.5)}{D_*^{0.3}} \quad (9)$$

in which d_{50} is the mean particle diameter, $\Delta = (\rho_s - \rho_w)/\rho_w$ is the relative density, $D_* = d_{50}(\Delta g/v^2)^{1/3}$ is the sedimentological diameter, ρ_s is the sediment density, ρ_w is the fluid density, g is the gravitational acceleration, v is the laminar kinetic viscosity and a is thickness of the reference bottom layer.

Computational results.

Some calculations are made using the above described boundary conditions and numerical models. In Figure 1 the evaluation of the bottom slope is represented, while in Figure 2 the turbulence energy and in Figure 3 the concentration are plotted for the last time step. The initial water depth is 13.6m, the inflow velocity is 0.5m/s, the roughness according to Nikuradse at the inflow boundary is 0.4m while the roughness at the erodible bed was 4.0m. Unfortunately, at the time of writing no comparison with the model of Hoffmans (1992) or experiments (Hoffmans, 1992) are available.

Acknowledgement.

The writer likes to thank Delft University for their support in providing computer facilities.

References.

- Graauw A.F.F. De, & K.W. Pilarczyk, 1981, Model-prototype conformity of local scour in non-cohesive sediments beneath overflow-dam, 19th IAHR-congress, New Delhi.
- Hoffmans, G.J.C.M., 1992, Two-dimensional mathematical modelling of local-scour holes. Doctoral thesis, Communication No. 92-7, Hydr. Geotechn. Engrg. Div., Delft Univ. of Technol., Delft.
- Kerssens, P.J.M., Prins, A. and L.C. Van Rijn, 1979, Model for suspended sediment transport, J. of Hydr. Div., ASCE, No. HY5, pp. 461-476.
- Rijn, L.C. Van, 1986, Mathematical modelling of suspended sediment in non-uniform flow., J. of Hydr. Engrg, No. 112.
- Rijn, L.C. Van, & K. Meijer, 1986, Three-dimensional modelling of suspended sediment transport for current and waves, Rep. Q250/Q432/H461, Delft Hydraulics, Delft.

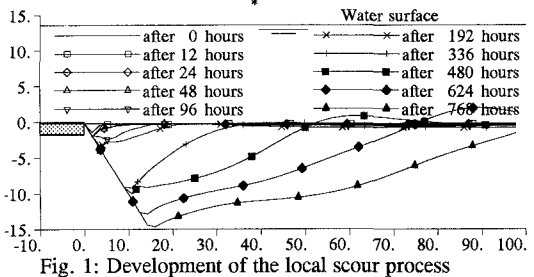


Fig. 1: Development of the local scour process

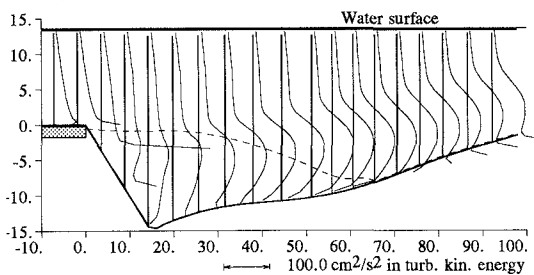


Fig. 2: Profiles of the turb. kin. energy at 768 hours

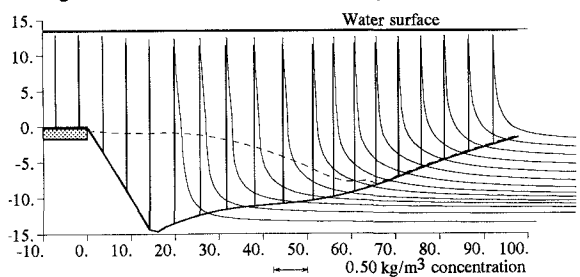


Fig. 3: Profiles of the sed. concentrations at 768 hours